

GLAUCOMA DIAGNOSIS OF MORPHOLOGICAL PROCESSING IN OPTICAL COHERENCE TOMOGRAPHY

T.R.Ganesh Babu¹, Dr.S.Senbaga Devi²,

¹Research Assistant, Department of Information and Communication Engineering, Anna University,
Chennai-600 025, India

²Assistant Professor, Department of Electronics and Communication Engineering, Anna University,
Chennai-600 025, India

Abstract. Glaucoma arises due to the inadequate fluid flow from the drainage canals of the eye. We propose an algorithm to automatically compute this accretion from the Optical coherence tomography (OCT). Ophthalmic imaging is the first application of OCT where it has proven particularly useful in diagnosing, monitoring, and studying glaucoma. Glaucoma often goes undetected until significant damage to the subject's visual field has occurred even when it is difficult. As Glaucoma progresses, neural tissues die, the nerve fiber layer thins, and the cup-to-disk ratio increases. Unfortunately, most current measurement techniques are subjective and inherently unreliable making it difficult to monitor small changes in the nerve head geometry. We present the algorithm to segment the retinal-nerve head surface, identify the choroid-nervehead boundary, and identify the extent of the optic cup. This algorithm was tested with many samples of OCT images from both normal and pathological eyes, and results were compared with experienced, expert ophthalmologist, reporting a correlation coefficient for cup to disk ratio.

Keywords: Glaucoma, Morphological processing, Optical Coherence Tomography, Optic cup, Optic disk, Optic nerve head.

1. Introduction

An imaging technique is Optical coherence tomography (OCT) similar to ultrasound[1]. OCT relies on the detection of backscattered light in what is essentially a Michelson interferometer to produce high resolution, cross-sectional images. OCT has been particularly useful in biological imaging applications such as dermatology, cardiology, and ophthalmology [2-4]. Among this, OCT has been used for a variety of purposes ranging from measuring corneal thickness in the anterior region of the eye to measuring the retinal thickness in the posterior [5]. OCT shows particular promise in detecting glaucoma, [6] a serious disease characterized by the destruction of the optic nerve and the retinal nerve fiber layer (RNFL), and which is the largest cause of preventable blindness in the World. Early detection is critical because damage incurred by the optic nerve and nerve fiber layer is irreversible. OCT can make highly accurate measurements of retinal thickness with micrometer resolution. [7,8]. Glaucoma is difficult to diagnose in a single clinical visit unless the patient's condition is already severe. Instead, careful monitoring over a period of time is often necessary to make an accurate diagnosis. It has been estimated that (remarkably) up to 40% of the nerve fiber layer can be destroyed before any significant vision loss occurs [9].

Changes in the optic nerve head can, therefore, serve as effective early indicators of Glaucoma and that treatment is warranted. Thus, there is a critical need for accurate and repeatable techniques to assess the optic nerve head [10].

A. Basic Anatomy of the Eye

The chamber of eye can be classified as anterior and posterior. The smaller anterior chamber is the space between the lens and the cornea and it is not taken into account. Vitreous humor [11] is a transparent, relatively homogeneous, viscous fluid present in the roughly spherical space between the retina and the lens at much larger posterior chamber. The tissue layer at the back of the posterior chamber, where light rays are focused and sensed is the retina. The top layer of the retina consists of nerve fibers and the photoreceptors (rods and cones). The photoreceptors are just below the nerve fibers. Choroid, which is a highly reflective layer of tissue behind the retina, and mostly composed of blood vessels that feed the back of the eye. The retinal area is called as optic disc. The nerve fiber layers converge to form the optic nerve in retina. Optic nerve exits at the back of the eye for connecting to the brain. The optic cup is the depression in the center of the optic disc.

B. System Overview

It shows a pair of typical OCT cross-sectional nerve head scans with the key anatomical structures and imaging parameters labeled in Fig. 1. The cup-to-disk ratio (the ratio of the optic cup area to the total area of the optic disk) is a popular measure used by ophthalmologists for assessing the health of the optic nerve head. Typically, this ratio is small for normal patients. That is, the cup area is much smaller than the disk area.

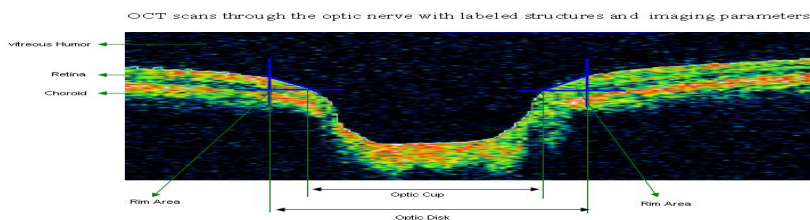


Fig.1: OCT image through optic nerve head with labeled structure

As Glaucoma progresses, more nerve tissue dies and the optic nerve shrinks causing the optic cup to sink and expand. Over time, the cup-to-disk ratio increases and the cup begins to deviate from its natural shape. The most common methods for assessing the cup-to-disk ratio are direct observation via an ophthalmoscope or a fundus image. This not only allows ophthalmologists to observe the color and shape of the nerve head but it also allows them to estimate the cup-to-disk ratio. In this paper we introduce a system to segment OCT nerve head images and extract its necessary parameter, the cup-to-disk ratio [14].

The basic steps of the system overview are given below as follows [12]:

- (i) Identifying the Retinal-Vitreous Boundary
- (ii) Identifying the Region of Retinal Choroid
- (iii) Identifying the edges of the Retinal Choroid boundary
- (iv) Calculation of cup to disk ratio Classification based on the obtained ratio

2. Retinal-Vitreous Boundary Detection

2.1. The Boundary Detection Algorithm

The boundary detection algorithm comprises four basic operations: Noise reduction, Optimal threshold selection, and Column wise edge detection. In this section, we consider each operation in turn, and present boundary detection results. The grey level OCT input image is first converted into binary image by applying Otsu's method. But due to the inherent noise present in the input image, the threshold image also has noise in it. To remove the unwanted information from the threshold image, median filter is applied.

1). Noise Reduction:

We use two different noise reduction methods, one for edge detection, which involves differentiation, and another for thresholding, which does not. To prepare the image for edge detection, the obtained binary image is used as the input for identifying the RVB. Initially 2D median filtering is performed to reduce speckle noise, the salt and pepper noise present in the image. Here we use 7x7 neighborhood [13].

2). Optimal threshold selection:

In our case, we remove the small objects present in the processed image morphological opening is done. Here we remove all small objects less than 1000 pixels. Disk shape morphological structural element of radius 5 is created and the processed image is dilated using the created structural element.

3). Column wise Edge Detection:

Column wise edge detection is done as follows. Edges of the resultant image are found by using sobel edge detection. Since we will find discontinuities in the identified boundary level - I, next level is obtained after improvement. For different patients, normal and abnormal images were taken and thus the retinal - vitreal boundary edges were detected.

3. Extracting Choroid

3.1. Retinal-vitreous boundary Choroid Preprocessing

Using the above obtained retinal-vitreous boundary image[15], two mask images are created. The width of the mask-1 is 20 and other is 100 (mask-1 is above 20 pixel from marked boundary region & mask-2 is below 100 pixels from the marked boundary region). Next the morphological structural element of line shape with width 2 and 90 degree's created. The input color image using the created structural element is eroded. We convert the input color image to gray scale image and then it is quantized to the number of gray level used from 256 to 8. From the quantized image, by applying Otsu thresholding method, binary image is obtained. Two dimensional (2D) median filtering is applied to reduce the salt and pepper noise present in the image. Here we use 7x7 neighborhood.

3.2. Retinal-vitreous boundary Choroid processing

Initially the region mask-2 is considered. The logical AND operation is performed with quantized median filtered binary image. The resultant image is performed with mask-1 by the logical OR operation and considered for further process.

- (i) Create the structural element of width two and degree zero and erode the processed image using the created structural element.
- (ii) First few and last few (say 5) column are also marked as one to close the regions present in the edge of the image.
- (iii) The unconnected pixels which have two non-zero neighbors that are not connected are connected.
- (iv) The regions boundaries present in the binary image are traced.
- (v) After calculating area of each region only the large region which is above 500 pixels are chosen as the region of interest for identifying the edge of the choroids.

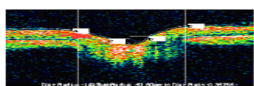
From the resultant image, the images are considered as two half sides. i.e., left and right. Find the indices X1, Y1 of the non-zero element present in the left half. Find the indices of the X2Y2 for right region. From the left half the right most column and particular row where the region bounding present, are identified. Similarly from the right half, the left most column and particular row where the region bounding present, are identified.

3.3. Identifying the Optic Disk Endpoints

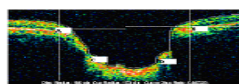
From the identified choroid edges horizontal and vertical lines are drawn and also the identified Retinal-Vitreous Boundary is marked in the same image. The two intersecting points between the horizontal drawn line and the Retinal-Vitreous Boundary is marked as C and D. The distance between two identified choroid edge gives the diameter of the optic disk. The distance between the point A and B is known as diameter of the cup.

4. Conclusion

Cup to Disk ratio is calculated as the ratio of the distance between A and B to the distance between C and D. The Calculation of cup to disk ratio is 0.30786 for normal image and 0.80526 for abnormal image.



(a) normal image



(b) Abnormal Image

Fig.2: Normal and Abnormal Images

From the above calculation, if the cup to disk ratio exceeds more than 0.3 it indicates that glaucoma is present. This method has been tried for one normal patient and for thirty patients affected by Glaucoma. For twenty five patients, the results have been identified correctly. Only results for ten patients have been tabulated. But for the remaining patients, due to the poor quality of the image, the choroidal region is not

identified properly. Hence error is seen in the cup to disc ratio. The calculated results coincide with the calculation done by Ophthalmologists.

PATIENT No	CUP TO DISC RATIO	
	LEFT EYE	RIGHT EYE
1	0.203	0.149

Table .1 NORMAL IMAGE

SL.NO	PATIENT No	CUP TO DISC RATIO	
		LEFT EYE	RIGHT EYE
1	1	0.61	0.635
2	2	0.71	0.601
3	3	0.76	0.89
4	4	0.611	0.427
5	5	0.782	0.82
6	6	0.677	0.566
7	7	0.796	0.608
8	8	0.84	0.34
9	9	0.65	0.534
10	10	0.75	0.739

Table . 2 ABNORMAL IMAGE

5. Acknowledgment

The authors wish to thank Dr. Rengaraj Venkatesh, M.D., Professor of the Aravind Eye Hospital & Post Graduate Institute of Ophthalmology, Pondicherry, India for providing the expert analysis of the OCT data.

6. References

- [1]. D. Huang, E. A. Swanson, and C. Lin et al., "Optical coherence tomography," *Science*, vol. 254, 1991, pp. 1178–1181.
- [2]. M. E. Brezinski, G. J. Tearney, and B. E. Brett, "Imaging of coronary artery microstructure with optical coherence tomography," *Am. J. Cardiol.*, vol. 77, 1996, pp. 92–93.
- [3]. M. R. Hee, J. A. Izatt, and E. A. Swanson et al., "Optical coherence tomography for ophthalmic imaging," *IEEE Eng. Med. Biol. Magazine.*, vol. 14, 1995, pp. 67–76.
- [4]. J. Welzel, E. Lankenau, R. Birngruber, and R. Engelhardt, "Optical coherence tomography of the human skin," *J. Am. Acad. Dermatol.*, vol. 37, 1997, pp. 958–963.
- [5]. R. Wang, D. Koozekanani, C. Roberts, and S. Katz, "Reproducibility of retinal thickness measurements using optical coherence tomography," *Invest. Ophthalmology Vis. Sci.*, vol. 40, 1999, pp. S125–S125.
- [6]. C. A. Puliafito, M. R. Hee, J. S. Schuman, and J. G. Fujimoto, "Optical Coherence Tomography of Ocular Diseases", Eds., 1st ed. Thorofare, NJ: Slack, 1996.
- [7]. L. Pieroth, J. Schuman, E. Hertzmark, M. Hee, J. Wilkins, J. Coker, C. Mattox, T. Pedut-Kloizman, C. Puliafito, J. Fujimoto, and E. Swanson, "Evaluation of focal defects of the nerve fiber layer using optical coherence tomography," *Ophthalmology*, vol. 106, no. 3, Mar. 1999, pp. 570–579.
- [8]. M. Pons, H. Ishikawa, R. Gürses-Özden, J. Liebmann, H. Dou, and R. Ritch, "Assessment of retinal nerve fiber layer internal reflectivity in eyes with and without glaucoma using optical coherence tomography," *Arch. Ophthalmology.*, vol. 118, Aug. 2000, pp. 1044–1047.
- [9]. B. F. Boyd and M. H. Luntz, "Innovations in the Glaucomas: Etiology, Diagnosis, and Management", 1st ed. El Dorado, Panama: Highlights of Ophthalmology Int., 2002.
- [10]. A. Mistlberger, J. Liebmann, D. Greenfield, M. Pons, S. Hoh, H. Ishikawa, and R. Ritch, "Heidelberg retina tomography and optical coherence tomography in normal, ocular-hypertensive and glaucomatous eyes," *Ophthalmology*, vol. 106, no. 10, Oct. 1999, pp. 2027–2032.
- [11]. W. Tasman and E. A. Jaeger, Eds. "The Willis Eye Hospital Atlas of Clinical Ophthalmology", 2nd ed. Philadelphia, PA: Lippincott/Williams & Wilkins, 2001.
- [12]. Kim L. Boyer, Artemas Herzog, and Cynthia Roberts, "Automatic Recovery of the Optic Nervehead Geometry in

Optical Coherence Tomography”, IEEE Transactions On Medical Imaging, VOL. 25, NO. 5, May 2006

- [13]. J. Rogowska and M. Brezinski, “Evaluation of the adaptive speckle suppression filter for coronary optical coherence tomography imaging,” IEEE Trans. Med. Imag., vol. 19, no. 12, Dec. 2000, pp. 1261–1266.
- [14]. D. Koozekanani, K. Boyer, and C. Roberts, “Retinal thickness measurements from optical coherence tomography using a Markov boundary model,” IEEE Trans. Med. Imag., vol. 20, no. 9, Sep. 2000, pp. 900–916.
- [15]. D. C. Cabrera Fernández, “Delineating fluid-filled region boundaries in optical coherence tomography images of the retina,” IEEE Trans. Med. Imag., vol. 24, no. 8, Aug. 2005, pp. 929–945.